Final Report

Magnetic Responsive Hydrogel material Delivery System II

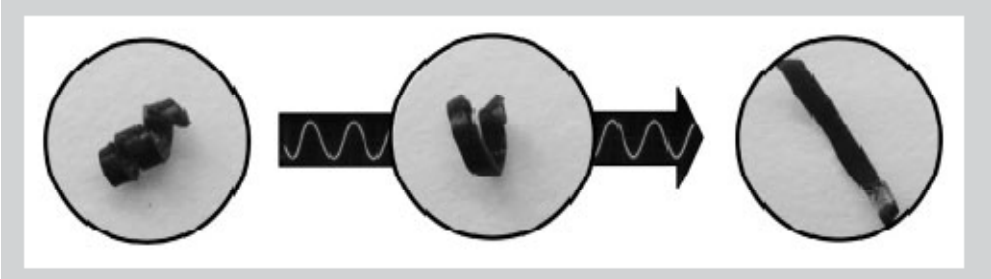

2010-08-10

by

Soo-Young Park

To Asia Office of Aerospace Research and Development

Department of Polymer Science, Kyungpook National University, 1370 Sankyuk-dong, Buk-gu,

Deagu 702-701, Republic of Korea.

Tel: +82-53-950-5630; Fax: +82-53-950-6623; e-mail: psy@knu.ac.kr

Report Documentation Page

Form Approved
OMB No. 0704-0188

1. REPORT DATE	2. REPORT TYPE	3. DATES COVERED
29 SEP 2010	**Final**	**17-06-2009 to 17-07-2010**

4. TITLE AND SUBTITLE
Magnetic responsive hydrogel material delivery system II

5a. CONTRACT NUMBER
FA23860914041

5b. GRANT NUMBER

5c. PROGRAM ELEMENT NUMBER

6. AUTHOR(S)
Soo-Young Park

5d. PROJECT NUMBER

5e. TASK NUMBER

5f. WORK UNIT NUMBER

7. PERFORMING ORGANIZATION NAME(S) AND ADDRESS(ES)
Kyungpook National University,#1370 Sangyuk-Dong, Buk-gu,Daegu 702-701,Korea (South),NA,NA

8. PERFORMING ORGANIZATION REPORT NUMBER
N/A

9. SPONSORING/MONITORING AGENCY NAME(S) AND ADDRESS(ES)
AOARD, UNIT 45002, APO, AP, 96337-5002

10. SPONSOR/MONITOR'S ACRONYM(S)
AOARD

11. SPONSOR/MONITOR'S REPORT NUMBER(S)
AOARD-094041

12. DISTRIBUTION/AVAILABILITY STATEMENT
Approved for public release; distribution unlimited

13. SUPPLEMENTARY NOTES

14. ABSTRACT

We have developed a novel route for the synthesis of the thermoresponsive core-shell nanoparticles that consist of the magnetite core and the poly(N-isoproplyacrylamide) (poly(NIPAAm) shell in aqueous medium. Magnetic nanoparticles (MNPs) were coated with first oleic acid (OA) and then vinyl carboxylic acid-β-cyclodextrin (MAH-β-CD). The OA-MNPs and the MAH-β-CD-MNPs showed mono-dispersion in a n-hexane and aqueous medium, respectively. NIPAAms were successfully polymerized from the vinyl double bonds of the MAH-β-CD MNPs and cross-linked with N, N-methylenebisacrylamide (MBA) to make the stable thermo-responsive core-shell morphology with the MNP core and the poly(NIPAAm) shell (poly(NIPAAm)-MNP). The aqueous solutions dispersed with poly (NIPAAm)-MNPs showed magnetic heating due to a super paramagnetic property, and the poly (NIPAAm) shell shrank above its LCST temperature. Apart from aqueous dispersed solution PNIPAAm magnetite composite film can also be prepared via photopolymerization using APS as a photo initiator. The film synthesized is cross linked with MBA and thus insoluble in water. When AC magnetic field is applied on such a PNIPAAm nanocomposite film, MNPS oscillate and produce heat and as a result PNIPAAm shrinkage can be observed. The combination of these properties are potentially important in target delivery of therapeutic agent in vivo, hyperthermic treatment of tumors, magnetic resonance imaging (MRI) as contrasting agents, tissue repair, immunoassay, cell separation, biomagnetic separation of biomolecules, etc.

15. SUBJECT TERMS

16. SECURITY CLASSIFICATION OF:			17. LIMITATION OF ABSTRACT	18. NUMBER OF PAGES	19a. NAME OF RESPONSIBLE PERSON
a. REPORT **unclassified**	b. ABSTRACT **unclassified**	c. THIS PAGE **unclassified**	**Same as Report (SAR)**	**23**	

Standard Form 298 (Rev. 8-98)
Prescribed by ANSI Std Z39-18

Abstract: We have developed a novel route for the synthesis of the thermoresponsive core-shell nanoparticles that consist of the magnetite core and the poly(N-isoproplyacrylamide) (poly(NIPAAm) shell in aqueous medium. Magnetic nanoparticles (MNPs) were coated with first oleic acid (OA) and then vinyl carboxylic acid-β-cyclodextrin (MAH-β-CD). The OA-MNPs and the MAH-β-CD-MNPs showed mono-dispersion in a n-hexane and aqueous medium, respectively. NIPAAms were successfully polymerized from the vinyl double bonds of the MAH-β-CD MNPs and cross-linked with N, N-methylenebisacrylamide (MBA) to make the stable thermo-responsive core-shell morphology with the MNP core and the poly(NIPAAm) shell (poly(NIPAAm)-MNP). The aqueous solutions dispersed with poly(NIPAAm)-MNPs showed magnetic heating due to a superparamagnetic property, and the poly(NIPAAm) shell shrank above its LCST temperature. Apart from aqueous dispersed solution PNIPAAm magnetite composite film can also be prepared via photopolymerization using APS as a photoinitiator. The film synthesized is crosslinked with MBA and thus insoluble in water. When AC magnetic field is applied on such a PNIPAAm nanocomposite film, MNPS oscillate and produce heat and as a result PNIPAAm shrinkage can be observed. The combination of these properties are potentially important in target delivery of therapeutic agent in *vivo*, hyperthermic treatment of tumors, magnetic resonance imaging (MRI) as contrasting agents, tissue repair, immunoassay, cell separation, biomagnetic separation of biomolecules, etc. The scheme for the synthesis of such type of study is shown below:

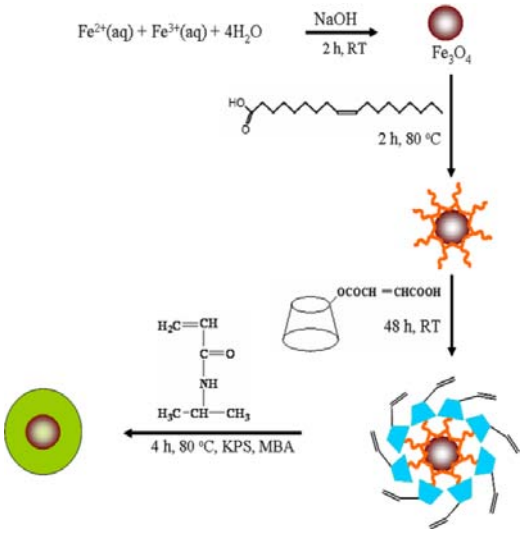

This work has been submitted to Journal of Materials Chemistry.

1. Introduction : In the past few years, considerable interest has been devoted towards the design of new drug delivery systems with an aim to release drug at a controlled rate and desired time.[1] MNPs have shown great potential for use in biomedicine due to their ability to get close to biological entities such as cells, viruses, proteins, and genes with heating ability when exposed to a time-varying magnetic field.[2] Superparamagnetic MNPs with proved biocompatibility[3] have attracted significant attention as drug carriers in hyperthermia therapy, magnetic resonance imagining (MRI) as a contrasting agent, tissue repair, immunoassay, and cell separation procedures.[4] A wide range of methods were proposed for the synthesis of iron and iron-based MNPs. Popovici et al., used a laser pyrolysis technique to produce iron-based nanomaterials.[5] Choi et al., synthesized MNPs by chemical vapor condensation and pyrolysis of organometallic precursors of $Fe(CO)_5$.[6] Xiaomin et al., developed a one-step route for the preparation of MNPs by reduction of iron salts with hydrazine hydrate in a strong alkaline solution.[7] Martínez-Mera et al., synthesized MNPs by a colloidal method at room temperature without the use of surfactants.[8]

Thermally-responsive polymers are an important class of responsive polymers with potential applications in biomedical fields, such as micro fluidic devices,[9] pulsatile drug release systems,[10-13] bioadhesion mediators [14,15] and motors/actuators.[16,17] Thermally-responsive polymers can collapse or expand on heating.[18] Poly(NIPAAm) collapses when the temperature increases above its LCST temperature. The phase transition in poly(NIPAAm) is due to the amphiphilic nature of the monomer unit itself. The balance between the hydrogen bonding interactions (between the hydrophilic -C=O and -NH groups) and the hydrophobic interactions (between pendant isopropyl groups) is instrumental in stabilizing poly(NIPAAm).[19] The major problem associated with MNPs is that they are usually dispersed in organic media. Not many studies have been reported in the literature on the synthesis of MNPs dispersible in aqueous medium. To potentially use MNPs in biomedical fields and to understand their implications, it is essential to develop a generic synthetic route which can transfer MNPs from an organic phase to an aqueous phase.

MNPs have found very useful applications in bioseparation, drug delivery system, hyperthermia for cancer therapy, and magnetic resonance imaging (MRI). [20-22] Ikkai et al [23,24] developed a novel UV-induced gelation method, by using ammonium persulfate (APS) as the UV-photoinitiator. APS can be used as a photoinitiator for the heat-induced and low-temperature redox polymerizations where the active radicals are generated by APS

dissociation. The UV-induced gelation method, in which APS can act as a UV-photoinitiator, is the important finding.[25]

Hybrid materials can be obtained by combining metal based nanoparticles e.g., gold (Au), silver (Ag) and iron (Fe) with polymer hydrogels for the synthesis of stable film formation. There is small effect on the mechanical properties of the resulting nanocomposite hydrogels by the addition of metallic nanoparticles as far as the interactions between polymer and nanoparticles are weak. Stronger polymer–nanoparticle interactions that are induced, e.g., by the attachment of gold reactive thiol groups to the poly(NIPAAm) hydrogel, may alter the thermosensitivity and swelling behavior. [26, 27] Using gold (Au) and silver (Ag), other nanoparticles such as iron (Fe), cobalt (Co), nickel (Ni), copper (Cu) and also metal alloys, salts, and metal-derived quantum dots (2–100 nm) can be mixed with or synthesized within a hydrogel matrix.[28,29] The applications of these hydrogels can be found in catalysis, sensors, actuators, and microfluidic devices and also in separation technology. However, only nontoxic and non hazardous biomaterials will find usage in the pharmaceutical and medical fields.[26] AC magnetic field produces magnetic rotations or alignments in response to a high-frequency magnetic field allow nanoparticles to heat up the surrounding hydrogel matrix in which they are trapped. Such remote heating could be used for inducing noninvasive focused hyperthermia, for controlled drug release, and for triggering thermosensitive changes in hydrogel volume or shape.[30, 31] Magnetic hydrogels thus offer ways to selectively target, detect, and potentially treat cancer tissue via magnetic resonance imaging (MRI) and inductive heating.[32]

The present work has developed a novel route for the synthesis of the aqueous-phase dispersible MNPs coated with the thermoresponsive polymer poly(NIPAAm). It is believed that this novel route for the synthesis of the thermoresponsive core-shell MNPs in aqueous medium (as shown in above scheme) will prove a potential step forward in the use of these core-shell MNPs in robust controlled drug delivery, tissue repair, immunoassay, cell separation, biomagnetic separation of biomolecules, etc.

2. Experimental

2.1 Preparation of poly(NIPAAm)-MNPs : Ferric chloride hexahydrate ($FeCl_3.6H_2O$), ferrous chloride tetrahydrate ($FeCl_2.4H_2O$), sodium hydroxide (NaOH), oleic acid (OA), maleic anhydride (MAH), benzene, n-hexane, N, N-dimethyl formamide (DMF), acetone (C_3H_6O), trichloromethane ($CHCl_3$) potassium persulfate (KPS) were purchased from Duksan©. β-cyclodextrin (β-CD), N-isopropylacrylamide (NIPAAm) and N, N-

methylenebisacrylamide (MBA) were purchased from Sigma Aldrich©. KPS and NIPAAm were recrystallized from water and a benzene/n-hexane (3:6 v/v) mixture, respectively. All the other chemicals were of analytical-reagent grade and were used as received. Magnetites were synthesized using the chemical co-precipitation method. Calculated amounts of $FeCl_2 \cdot 4H_2O$ and $FeCl_3 \cdot 6H_2O$ in grams were dissolved into deionized water. A three necked flask was charged with 100 mL of 2 $mol \cdot L^{-1}$ NaOH solution. The solution of Fe^{+2}/Fe^{+3} was added dropwise to the NaOH solution and the mixture solution was vigorously stirred over a period of 2 h. The resulting MNPs were washed repeatedly with first deionized water and then ethanol, dried in a vacuum oven at 50 ^oC for 12 h, and stored in glass vials.

Figure 1. Digital image of the synthesis of magnetic nanoparticles (MNPs).

To obtain the OA-modified MNPs (OA-MNPs), calculated amounts of MNPs were sonicated in deionized water for 1 h. 13 mL of OA per gram of MNPs were added dropwise into the MNP-dispersed water at 80 ^oC over the course of 2 h under vigorous mechanical stirring and nitrogen atmosphere. After modification, the MNPs were extracted into n-hexane and washed repeatedly with first water and then ethanol to remove the unreacted OAs. The introduction of MAH in β-CD was performed according to the reported method [33] as follows. A 5.68 g of β-CD (0.005 mol) was dissolved in 30 mL DMF, and then 4.90 g of MAH (0.05 mol) was added to it. The solution was heated at 80 ^oC under vigorous stirring for 10 h. When the reaction was completed, the solution was cooled at room

temperature and 30 mL of trichloromethane were added to it. White precipitates of MAH-β-CD were filtered, washed three times with acetone, dried in a vacuum oven at 40 ^{o}C for 24 h, and stored in a glass vial. For the coating of the OA-MNPs with MAH-β-CD (MAH-β-CD-MNPs), equal volumes of the OA-MNPs n-hexane solution (2 wt %) and the MAH-β-CD aqueous solution (2 wt %) were mechanically stirred at room temperature for 48 h. The OA-MNPs were transferred into the MAH-β-CD aqueous solution to make the MAH-β-CD-MNPs (the details will be discussed in the results and discussion section).[34] The MAH-β-CD-MNP powders were obtained by drying the aqueous part of the phase-separated n-hexane/water solution. The MAH-β-CD-MNPs were used to make the thermoresponsive core-shell MNPs that consist of the magnetite core and the poly(NIPAAm) shell (poly(NIPAAm)-MNPs) by using a precipitation polymerization method in the presence of KPS (as an initiator) and MBA (as a cross-linker) under nitrogen atmosphere at 70^{o}C.[35] The mixture was cooled to room temperature and diluted with distilled water. The poly(NIPAAm)-MNPs were isolated from the solution by placing a magnet below the reaction vial. This process was repeated several times to remove the unreacted NIPAAm monomers and the separated poly(NIPAAm) chains from the MNPs.

2.2. Characterization : FT-IR spectra were obtained with a Nicolet-560 spectrometer on KBr pellets. X-ray diffraction (XRD) patterns of the MNPs were recorded using a X-ray diffractometer (D/max-Ra, Rigaku, Japan) with Cu-K_{α} radiation at 42 kV and 109 mA. The crystal size of MNPs was calculated using a Scherrer's equation (Eq.1) where β is the width of the peak at half maximum intensity of a specific (hkl) diffraction peak in radians, K is a constant of 0.9, λ is the wavelength of the incident X-ray, θ is the half angle between the incident and diffracted beams (2θ), and L is the crystallite size.

$$L = \frac{K\lambda}{\beta \cos\theta} \text{ ----------(1)}$$

The magnetic properties of the synthesized MNPs were measured by using a lakeshore 7400 vibrating-sample magnetometer (VSM) at room temperature. The morphologies of the as-synthesized MNPs, the OA-MNPs, the MAH-β-CD-MNPs, and the poly(NIPAAm)-MNPs were studied using transmission electron microscopy (TEM, JEM-1OOCX, JEOL, Japan) with an accelerating voltage of 80 kV. Samples for TEM were prepared by dispersing

the MNPs in acetone at a very dilute concentration, dropping the dispersed solution on the carbon-coated copper grid, and then evaporating it. Poly(NIPAAm) was negatively stained with phosphotungstic acid in order to make the polymer part visible. (Negative staining solution was prepared by dissolving 0.1g (1 wt%) of sodium phosphotungstate (PTA) powder to 10 ml of distilled water in a shell vial). The pH of the solution was adjusted to 7.2 - 7.4 with the 0.1 N NaOH. The particle size of the OA-MNPs, MAH-β-CD-MNPs, and poly(NIPAAm)-MNPs were measured by taking into consideration upto ten (10) particles each from OA-MNPs, MAH-β-CD-MNPs, and poly(NIPAAm)-MNPs, determined their diameter and then find out their mean value in nm. TGA thermograms were obtained in a nitrogen atmosphere at a heating rate of 10 ^{o}C/min between 25 ^{o}C and 600 ^{o}C using a TA 4000/Auto DSC 2910 System. The induction heating was measured with HF Induction Heater at 293 kHz and 2.5 kW with 4 mL and 2g/L solutions in which the weight of the MNPs from TGA results were considered for calculating the concentration of the solutions in the case of the organic material coated MNPs such as the OA-MNP and the poly (NIPAAm)-MNP. The hydrodynamic radius (R_h) of the poly(NIPAAm)-MNPs was measured with a dynamic light scattering (DLS) method (ELS-8000, Photal Otsuka electronics) at a wavelength of 632.8 nm (helium neon laser) from 22^{o}C to 68 ^{o}C with an increment of 2 ^{o}C. The concentration of the poly(NIPAAm)-MNP solution was 0.06 wt%, and the sample was sonicated before DLS measurement.

3. Results and discussion

3.1. Preparation of MNPs : The MNPs were synthesized with different Fe^{+2}/Fe^{+3} ratios as given in Table 1. The Fe^{+2}/Fe^{+3} ratios of S1, S2, and S3 in mol·L^{-1} (M) are 0.05/0.1, 0.1/0.2, and 0.5/1, respectively (As Fe_3o_4 can be synthesized by a molar ratio of 1:2 of ferrous and ferric salts. therefore, same ratio (1 : 2) has been kept for the concentration of Fe^{+2} and Fe^{+3}). Figure 2a shows the FT-IR spectra of the synthesized MNPs. As-synthesized MNPs showed bands at 570 and 630 cm^{-1} corresponding to the absorption bands of the Fe-O bond in the crystalline lattice, indicating that MNPs were successfully synthesized.[36] Figure 2b represents the XRD patterns of the S1, S2, and S3 with seven strong Bragg diffraction peaks, which can be indexed as (220), (311), (400), (422), (511), (440), and (533) of magnetite (Fe_3O_4) in a cubic phase.[37] The crystal size of MNPs (calculated from the most intense (311) peak increased with an increase in the Fe^{+2}/ Fe^{+3} molar ratio (Table 1). Due to concentration effects the particle size

has increased, also the same concentration ratio (1:2) has been kept throughout the synthesis of MNPs as Molar ratio for Fe^{+2} and Fe^{+3} is also same as 1:2. Figure 2c illustrates the magnetization curves of the S1, S2, and S3. The saturation magnetization (M_s) increased with an increase in the crystal size of the particles. The undetectable hysteresis and coercivity suggests that the synthesized MNPs have super paramagnetic properties. The S3 MNPs showed higher M_s compared to S1 and S2, therefore, S3 MNPs were used.

Table 1. Crystal size and magnetic properties of S1, S2, and S3 determined from X-ray and VSM. Ms is saturation magnetization, the values for coercivity (Hc) are given.

Sample	Fe^{+2} (M)	Fe^{+3} (M)	Particle size (nm)	M_s ($emu.g^{-1}$)	Hc (Oe)
S1	0.05	0.1	8.6	67.0	53.57
S2	0.1	0.2	10.7	67.0	57.40
S3	0.5	1.0	14.9	80.0	74.69

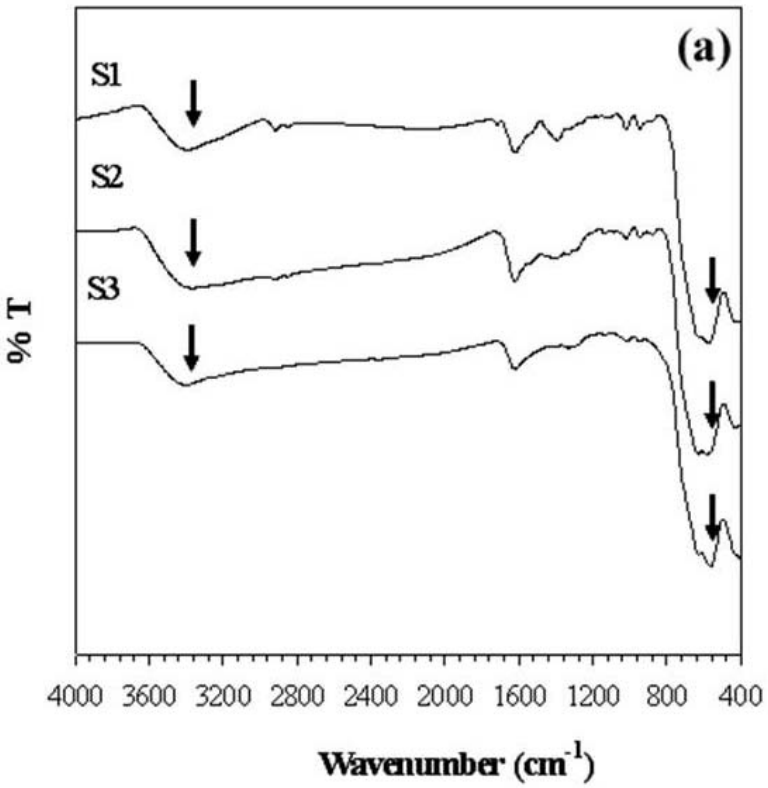
(a)
S1
S2
S3
% T
4000 3600 3200 2800 2400 2000 1600 1200 800 400
Wavenumber (cm-1)

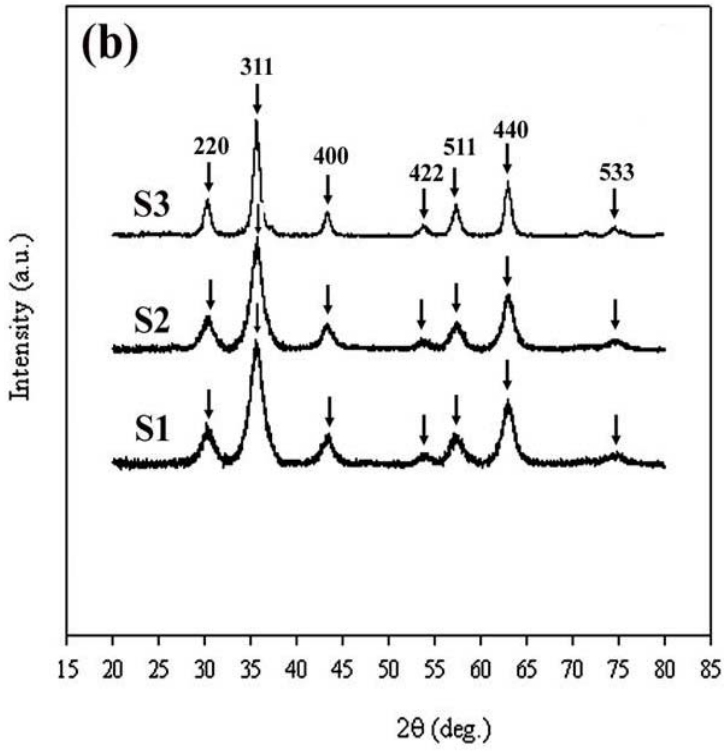
(b)
311
220
400
422
511
440
533
S3
S2
S1
Intensity (a.u.)
15 20 25 30 35 40 45 50 55 60 65 70 75 80 85
2θ (deg.)

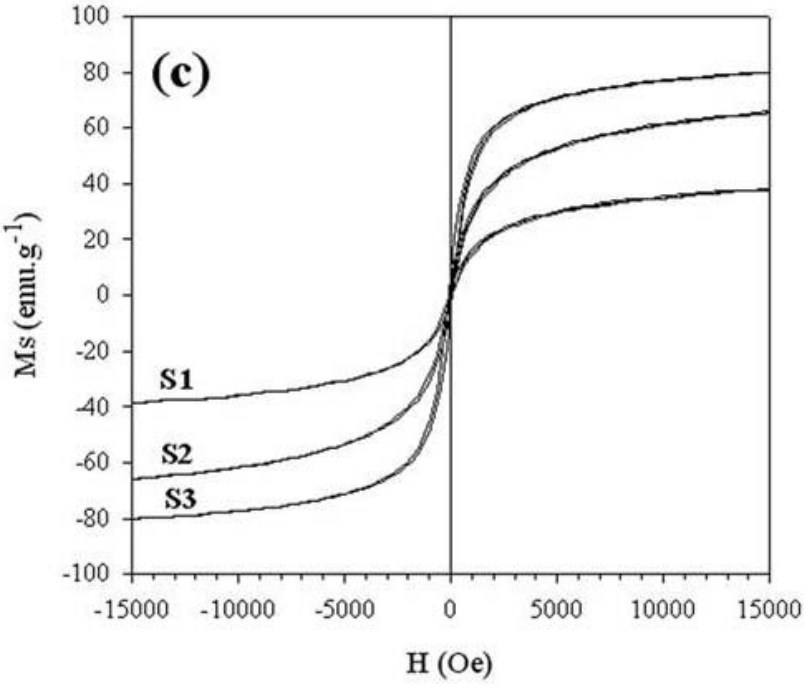

Figure 2. (a) FT-IR spectra of MNPs, (b) X-ray diffraction patterns, and (c) magnetization curves of the S1, S2 and S3 MNPs at room temperature where Ms is the saturation magnetization and H is the magnetic field strength.

3.2. Structure of MNPs : Figure 2a shows the FT-IR spectra of the OA, the OA-MNPs, the β-CD, the MAH-β-CD, and the Poly(NIPAAm)-MNPs. The FT-IR spectrum of the OA showed broad bands at 3500 and 2500 cm^{-1} due to the O-H stretching of carboxylic acid, and the bands at 1700, 1285, 1400, 2900, and 2800 cm^{-1} which were attributed to the C=O, C-O, COO^-, asymmetric CH_2, and symmetric CH_2 stretchings, respectively.[38] The OA-MNPs spectrum showed the O-H and COO^- stretching bands at 3500 and 1400 cm^{-1}, respectively, as well as the MNP bands (the absorption bands of the Fe-O bond, Figure 1a) at 570 and 630 cm^{-1}. The C-O stretching band at 1285 cm^{-1} in OA was shifted to the lower wave number of 1187 cm^{-1} due to the chemisorptions of OA (as an oleate $C_{17}H_{33}COO^-$) on the surface of the MNPs,[39] although the consistent C=O stretching band at 1700 cm^{-1} indicates the presence of some uncoated OA molecules.[33] In the spectra of β-CD and MAH-β-CD, the –OH band at 3200 cm^{-1} in β-CD was shifted to 3500 cm^{-1} in MAH-β-CD as a result of the introduction of MAH.[33] The intensity of the $-CH_2$-OH stretching band at 2900 cm^{-1} in β-CD was reduced in MAH-β-CD because $-CH_2$-OH groups were reacted with MAH.[33] New -COOH and C=O stretching bands at 2560 and 1720 cm^{-1}, respectively, also appeared in MAH-β-CD. The shift of –OH band, the reduction in intensity of the $-CH_2$-OH stretching bands, and the appearance of new –

COOH and C=O bands in the spectrum of MAH-β-CD confirmed the successful synthesis of MAH-β-CD. The FT-IR spectrum of the poly(NIPAAm)-MNP showed the characteristic poly(NIPAAm) bands (at 3300 cm^{-1} (broad secondary NH amide), 2971-2861 cm^{-1} (CH group in isopropyl group), 1649 cm^{-1} (strong C=O amide), 1541 cm^{-1} (strong NH amide II), 1458 cm^{-1} (-CH_2 scissoring vibration), 1385 cm^{-1} (-CH_3 bending vibration), 1365 cm^{-1} (C-H bending vibration), and 1170 cm^{-1} (bending vibration)) as well as the characteristic hydrolysed MAH (~1707 cm^{-1}) and the Fe-O bands (570 cm^{-1}). All these bands confirmed the successful synthesis of poly(NIPAAm)-MNP. Figure 2 shows the schematic (Figure 2b) and the digital image (Figure 2c) of the MNPs in the n-hexane/water mixture solution before and after mechanical stirring during which the brownish color gradually disappeared from the top n-hexane layer, then the aqueous layer became brownish, and finally the bottom layer ended up as a suspension. This phase transfer did not occur in a control experiment without MAH-β-CD, indicating that the MAH-β-CD formed an inclusion complex with the OA, and the hydrophilic groups in the β-CD made the β-CD-MNPs hydrophilic and dispersible in aqueous medium.[34]

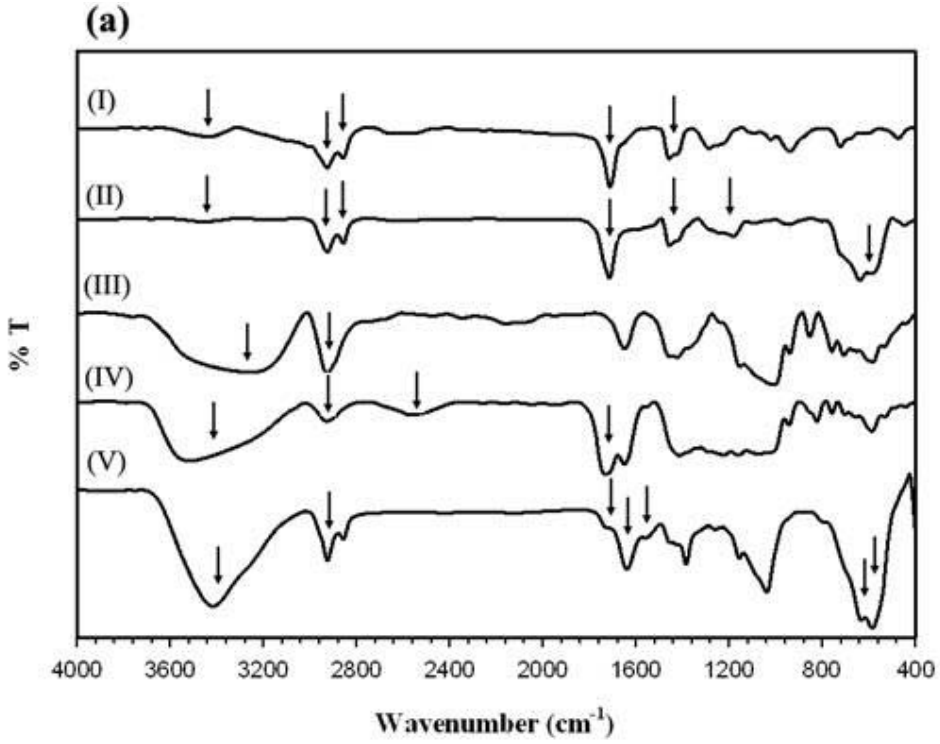

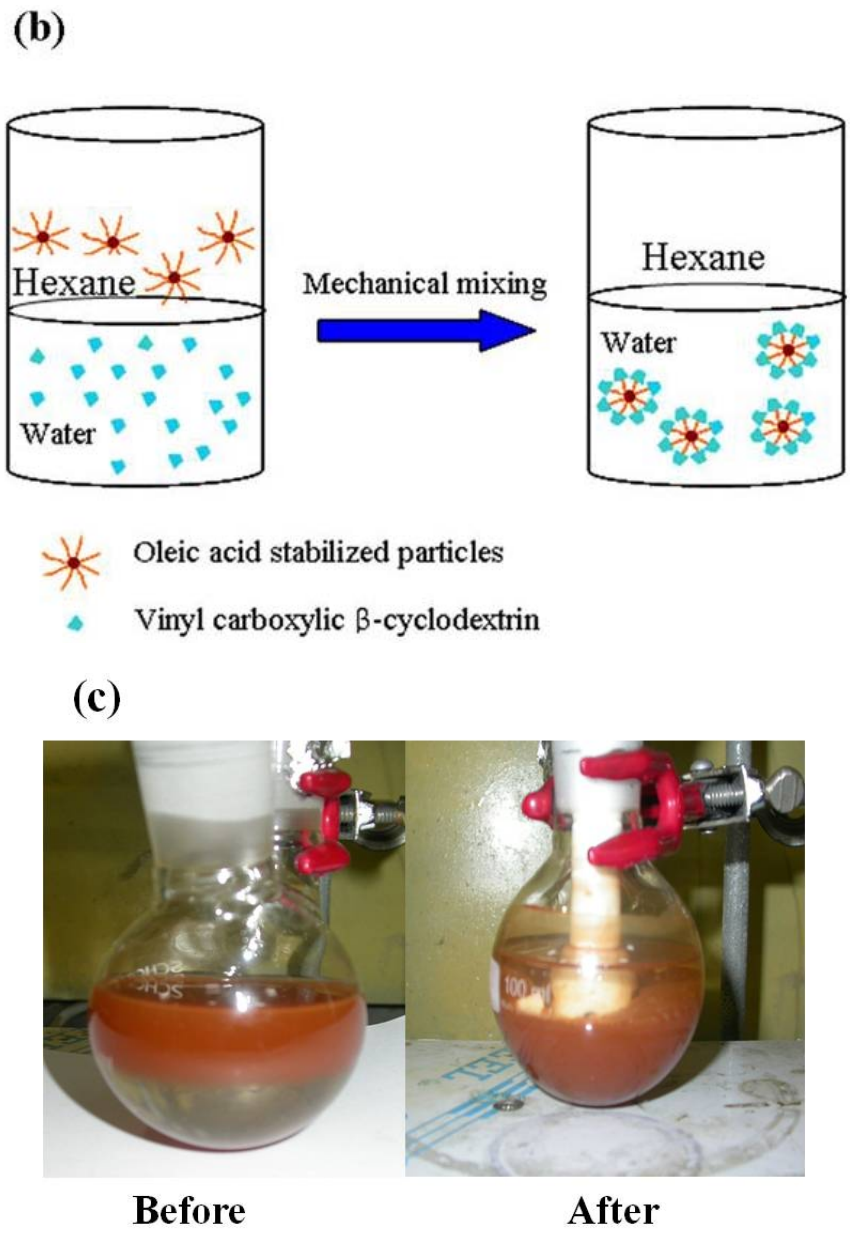

Figure 3. (a) FT-IR spectra of the (I) OA, (II) the OA-MNPs, (III) the β-CD, (IV) the MAH-β-CD, and (V) the poly(NIPAAm)-MNPs, (b) the schematic, and (c) the digital image of the phase transfer of S3 MNPs from an organic phase to an aqueous phase.

Figure 4 shows the TEM micrographs of the dispersed OA-MNPs in n-hexane, MAH-β-CD-MNPs and poly(NIPAAm)-MNPs in distilled water. The sizes of OA-MNPs, MAH-β-CD-MNPs, and poly(NIPAAm)-MNPs were narrowly distributed with a mean diameter of 41.8, 57.2, 85.6 nm, respectively. Standard deviation of the

particles (OA-MNPs, MAH-β-CD-MNPs, and poly(NIPAAm)-MNPs) was calculated and was found to be 4.744, 14.860, and 30.670 for OA-MNPs, MAH-β-CD-MNPs, and poly(NIPAAm)-MNPs, respectively. The clear image of poly(NIPAAm) surrounding MNPs was observed indicating the successful synthesis of poly(NIPAAm)-MNPs although some aggregations between poly(NIPAAm)-MNPs were observed. This aggregation could happen during the evaporating of the solvent on the TEM grids although there were also possibilities of the aggregated form during the synthesis. However, a similar morphology for the polymer-coated MNPs were reported by wang et al.[40]

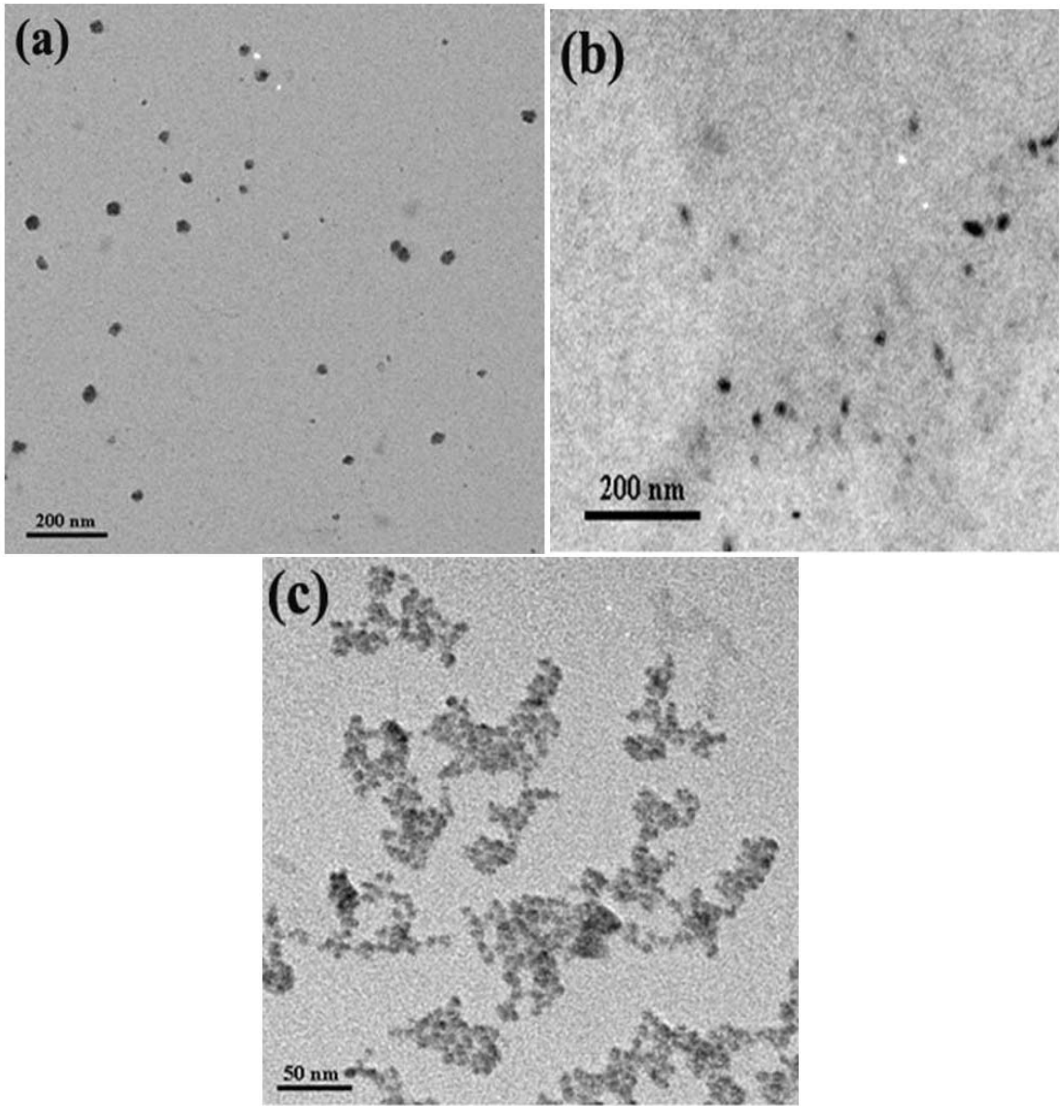

Figure 4. TEM micrographs of (a) OA-MNPs, (b) MAH-β-CD-MNPs, and (c) poly(NIPAAm)-MNPs.

The samples were prepared by dispersing OA-MNPs in n-hexane and MAH-β-CD-MNPs and poly(NIPAAm)-MNPs in distilled water. The dispersed samples were dropped on to a graphite coated copper grid and the solvent was allowed to evaporate. Poly(NIPAAm)-MNPs were stained with phosphotungstic acid.

Figure 5 shows the TGA thermograms of the MNPs, the OA-MNPs, and the poly(NIPAAm)-MNPs. The MNPs did not show any weight loss whereas the OA-MNPs and the poly(NIPAAm)-MNPs showed step-wise weight loss as temperature is increased. The weight losses of the OA-MNPs at ~ 250 and ~ 350 ^{o}C might be due to the thermal degradations of the free and coated OAs, respectively and those of the poly(NIPAAm)-MNPs at ~ 220 and ~ 350 ^{o}C might be due to the thermal degradations of the MAH-β-CD inclusion complex and the poly(NIPAAm), respectively.[41,42] These results also indicate the successful polymerization of poly(NIPAAm) onto the MNP surface.

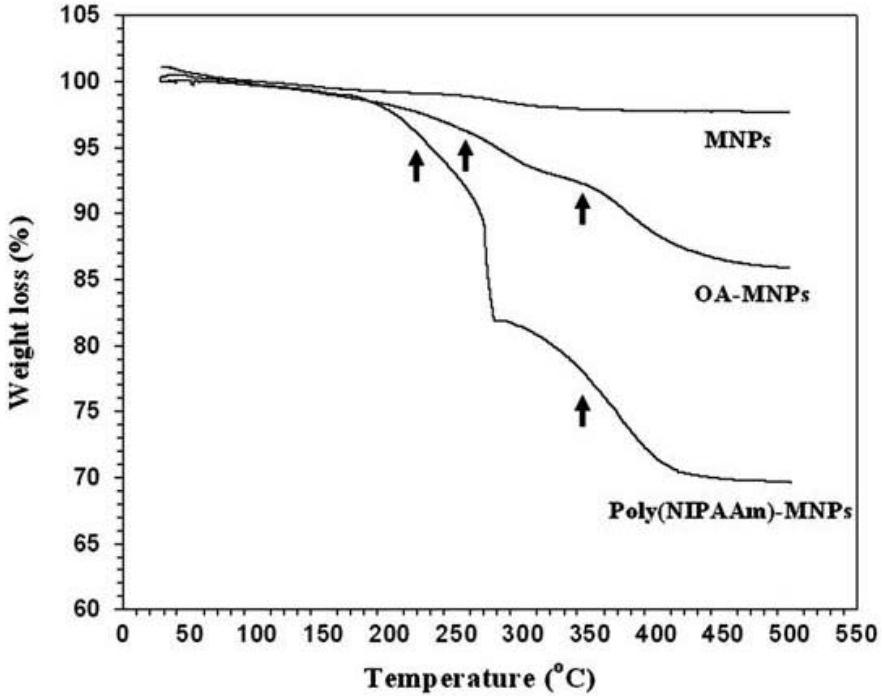

Figure 5. TGA thermograms of the MNPs, the OA-MNPs and the poly(NIPAAm)-MNPs.

3.3. Properties of MNPs : Figure 6a shows the temperature changes of the MNP (in 1M HNO_3), the OA-MNP (in hexane), and the poly(NIPAAm)-MNP (in water) in the oscillating magnetic field as a function of time. The temperature linearly increased initially and then saturated as time increased further. The temperature increase in the solutions indicates that the MNP particles have an ability of magnetic heating when exposed to an alternating

magnetic field.[43] The saturated temperatures of the MNPs, the OA-MNPs, and the poly(NIPAAm)-MNPs solutions were 65, 49, and 52 ^{o}C, respectively. The decrease of the saturation temperatures of the OA-MNPs and the poly(NIPAAm)-MNPs solutions as compared to that of the MNP might be due to low electrical conductivity of the organic shell (OA and poly(NIPAAm)).[44] Figure 6b shows the reversible attraction of the poly(NIPAAm)-MNPs toward a magnet. The poly(NIPAAm)-MNPs were homogeneous dark brown without magnet (Figure 6b(I)). However, the poly(NIPAAm)-MNPs were attracted toward the magnet when it was close to the wall of the vial (Figure 6b(II)) indicating a superparamagnetic property for the poly(NIPAAm)-MNPs. Superparamagnetic and magnetic heating properties of the poly(NIPAAm)-MNPs are critical for their applications in biomedical and bioengineering fields, because they prevent MNPs from aggregation and enables them to redisperse when the magnetic field is removed.[45] Figure 6c shows the thermo-responsive behavior of the poly(NIPAAm)-MNPs. The decrease in the hydrodynamic radii (R_h) happened at ~34 °C (LCST temperature of poly(NIPAAm)).[46] The decrease in radius at elevated temperature was due to the increased hydrophobicity of the poly(NIPAAm) segments, which led to the collapse of polymer chains and shrinkage of the gel network. Thus, this result indicates that the method developed might be one of the novel ways of synthesizing a thermo-responsive poly(NIPAAm)-MNPs which shows magnetic heating by MNPs in the core causing the shrinkage of the poly(NIPAAm) chains in the shell.

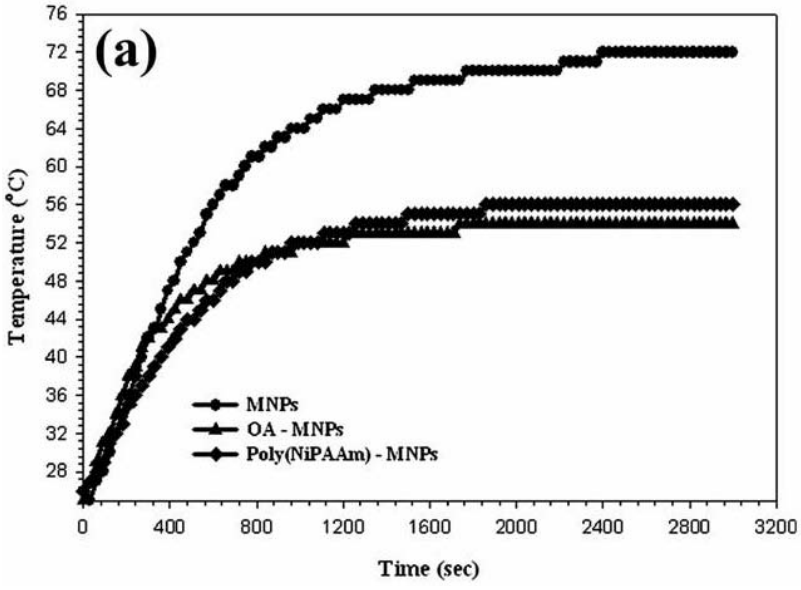

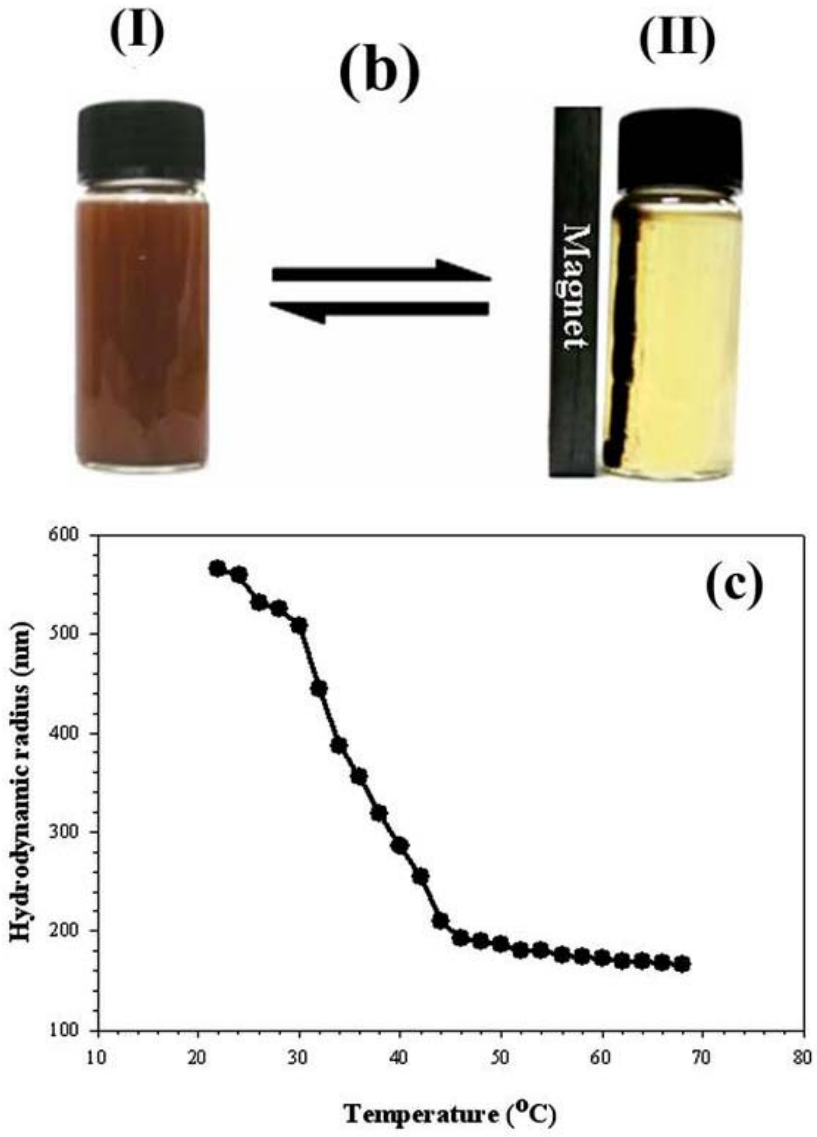

Figure 6. (a) The temperature changes of the MNP (in 1M HNO_3), the OA-MNP (in hexane), and the poly(NIPAAm)-MNP (in water) in the oscillating magnetic field as a function of time, (b) digital images of poly (NIPAAm)-MNPs in aqueous solution (I) without and (II) with magnet, and (c) hydrodynamic radii of the poly (NIPAAm)-MNPs dispersed in distilled water.

4. PNIPAAm composite film synthesis: Poly(NIPAAm) composite film was prepared by insitu photopolymerization of NIPAAm (0.5g), APS (0.01g; 2wt% with respect to NIPAAm), MBA (0.01 g; 2wt% with respect to NIPAAm) and modified MNPs (0.01g), known quantities in a small volume of water [47] i.e., 4 mL in a

small vial was taken and sonicated well before photopolymerization for a short period of time (2 to 3 minutes). Nitrogen gas was purged for 5 minutes. Solution was then poured into a petri dish and initially heated on a heating plate keeping the temperature between 40 to 50^{o}C for 5 minutes. Photopolymerization was carried out using UV irradiation upto 20 minutes. After UV irradiation for desired period of time PNIPAAm film prepared slowly and gradually. Washed with distilled water so as to remove the unreacted compounds. PNIPAAm film synthesis via photopolymerization can be seen in the following figure:

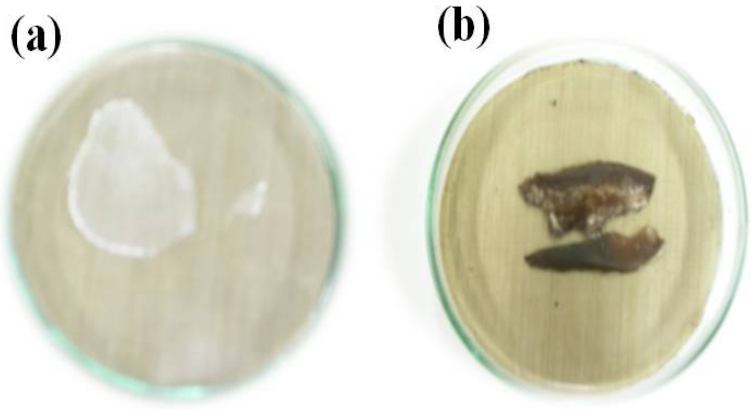

Figure 7. Digital images of PNIPAAm film formation via photopolymerization **(a)** Pure PNIPAAm film **(b)** PNIPAAm magnetite composite film.

4.1. Mechanism of Photopolymerization : The photoinitiator works with the ultraviolet (UV) light, when light of lower wavelength, less than 300 nm (190 to 220 nm) is exposed on to the polymerization mixture, the photoinitiator absorbs that light and is dissociated to produce radicals, which are very reactive, this whole process can be shown below:

Photoinitiator (I) when exposed to UV light decomposes, produces radicals and these reactive radicals (I*) further react with the monomers (R, R*) to start the photopolymerization as depicted below:

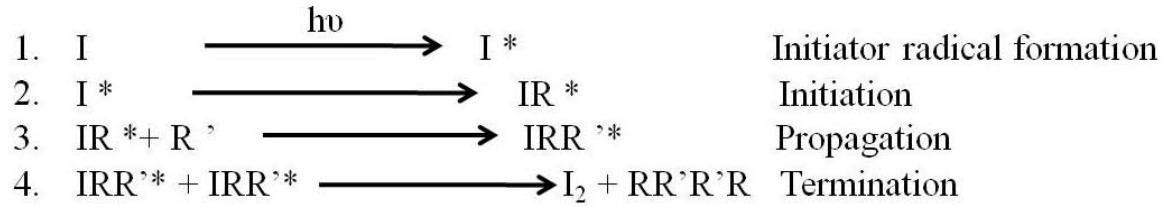

With the initiator radical formation, initiation and after that propagation of this process starts and when all the monomers are being consumed so the polymerization reaction terminates.

Schematically it can be shown in the following diagram:

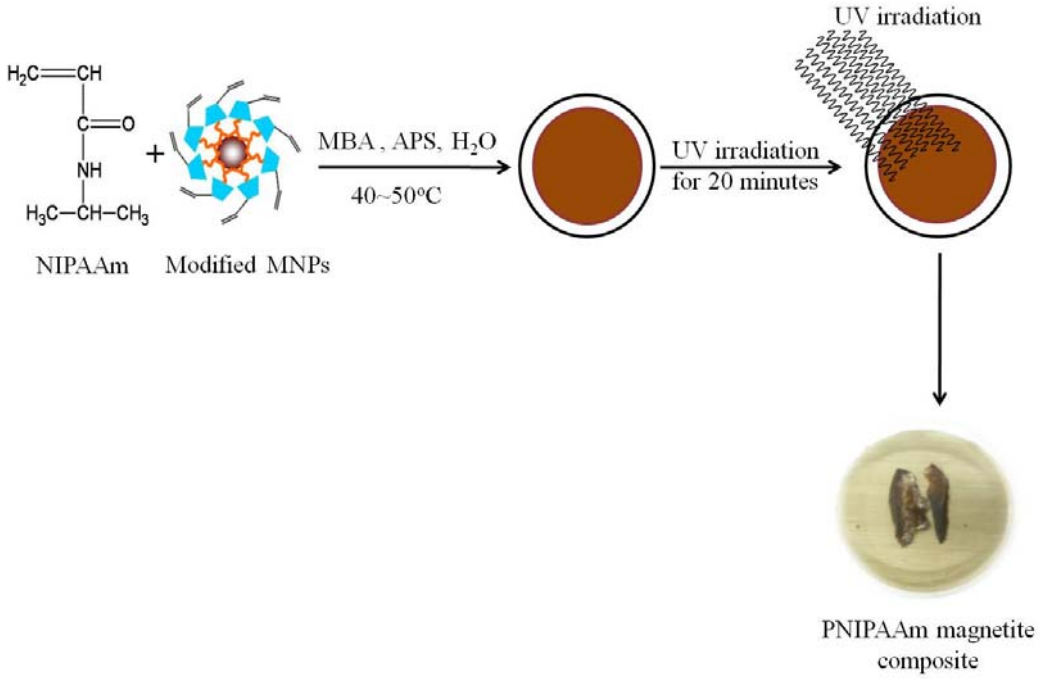

Figure 8. Schemetically showing the UV irradiation and PNIPAAm magnetite composite film formation.

The persulphate free radicals formed convert acrylamide monomers to free radicals which react with unactivated monomers to begin the polymerization chain reaction. The elongating polymer chains are randomly crosslinked by

MBA (crosslinker), resulting in a gel with a characteristic porosity which depends on the polymerization conditions and monomer concentration.

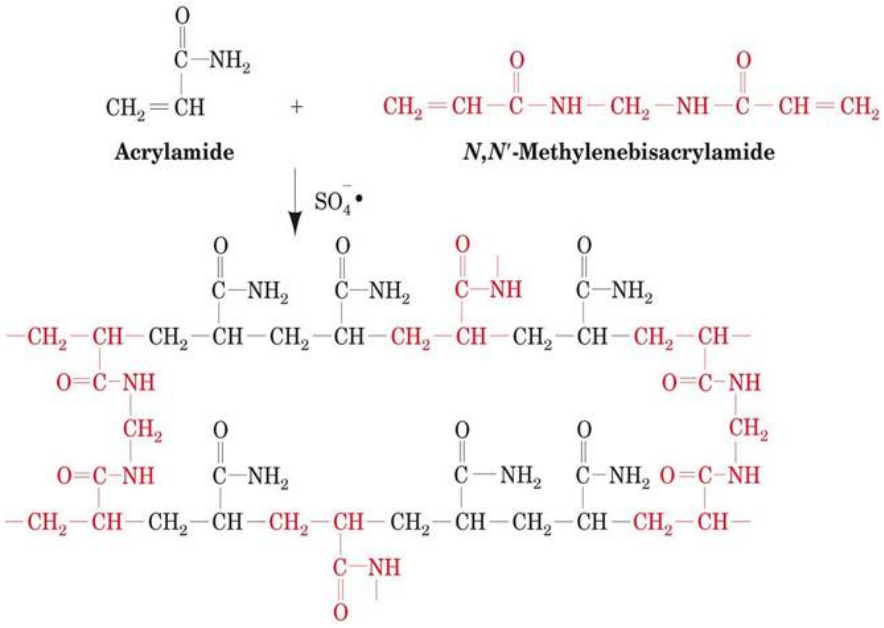

Figure 9. Crosslinking mechanism of acrylamide using MBA as a crosslinker, APS as a photoinitiator, its radical formation and the crosslinked acrylamide structure.

The shrinkage and swelling behavior of magnetite PNIPAAm composite film can be illustrated in the following figure as a function of AC magnetic field. When the field is OFF PNIPAAm is in swollen form, but when the field is turned ON, due to oscillation of MNPs heat is produced and consequently PNIPAAm shrinks and if it is in the form of a film so bending behavior due to shrinkage can be observed as in figure 10 (a). Typical PNIPAAm shrinkage can be seen in figure 10 (c) at above its LCST temperature i.e., 32 ^{o}C with the release of water molecules.

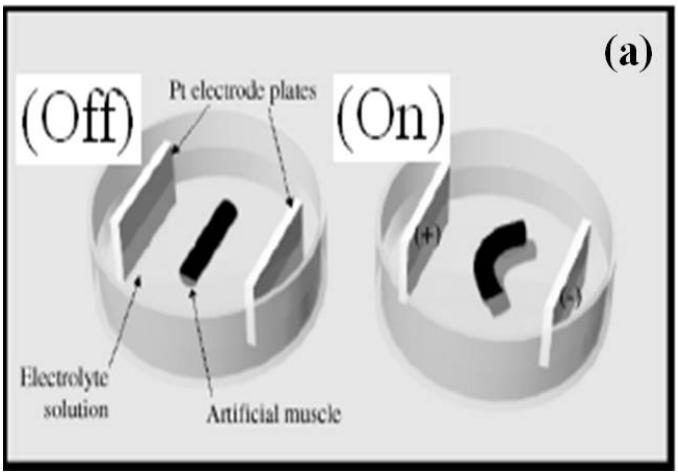

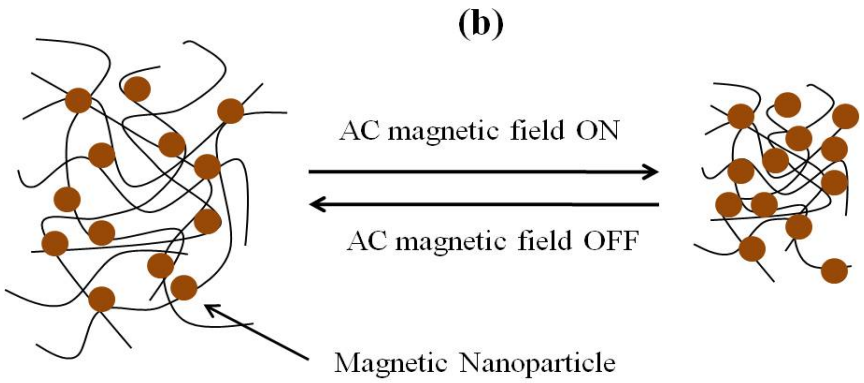

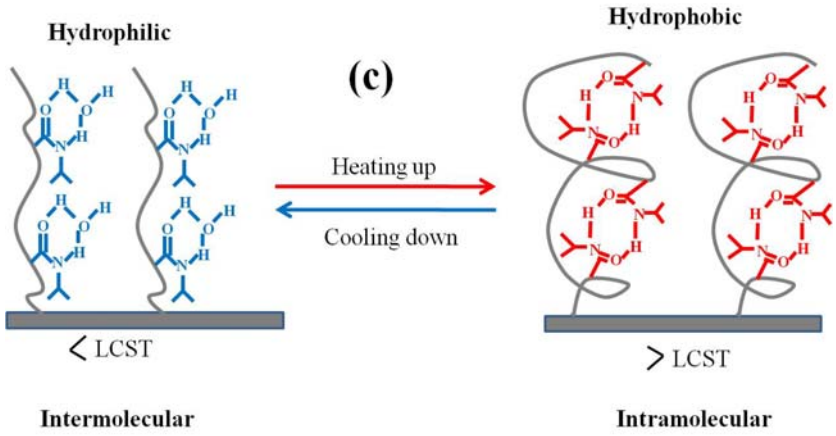

Figure 10. (a) Artificial muscle (hydrogel) response, demonstration to electric potential**. (b)** Proposed scheme for PNIPAAm magnetite composite shrinkage due to application of AC magnetic field. (from coil to globule structure). **(c)** PNIPAAm swelling and shrinkage below and above its LCST temperature.

5. Conclusions : This study has successfully prepared MNPs *via* a co-precipitation method in order to attach the poly(NIPAAm) chains on the MNPs to make the thermo-responsive core-shell MNPs. The MAH-modified β-CD where β-CD made an inclusion complex with OA which was first coated on MNP was introduced. The double bonds of the MAH in (MAH- β-CD) initiated the polymerization of NIPAAm and the poly(NIPAAm) chains in the shell were cross-linked with MBA. It is theorized that this novel approach for the preparation of the aqueous-dispersible thermoresponsive MNPs could be a step forward in their use in the fields of biomedical and bioengineering. Apart from aqueous dispersible thermoresponsive MNPs, a composite film of PNIPAAm and magnetite can also be made by using the photoinitiator as APS and UV irradiation, which can show thermoresponsive property in AC magnetic field.

References

1 J. Zhang and R. D. K. Misra, Acta Biomater., 2007, 3, 838.

2 Q. A. Pankhurst, J. Connolly, S. K. Jones and J. Dobson, J. Phys. D: Appl. Phys., 2003, 36, R167-R181.

3 U. Schwertmann and R. M. Cornell, Iron oxides in the laboratory: preparation and characterization., Weinh eim, Cambridge: VCH; 1991.

4 D. H. Kim, S. H. Lee, K. H. Im. K. N. Kim, K. M. Kim, I. B. Shim, M. H. Lee and Y. K. Lee, Curr. Appl. P hys., 2006, 6S1, e242.

5 E. Popovici, F. Dumitrache, I. Morjan, R. Alexandrescu, V. Ciupina, G. Prodan, L. Vekas and D. Bica, App l. Surf. Sci., 2007, 254, 1048.

6 C. J. Choi, O. Tolochko and B. K. Kim, Mater. Lett., 2002, 56, 289.

7 N. Xiaomin, S. Xiaobo, Z. Huagui, Z. Dongen, Y. Dandan and Z. Qingbiao, J. Crystal Growth., 2005, 275, 548.

8 I. Martínez-Mera, M.E. Espinosa-Pesqueira, R. Pérez-Hernández and J. Arenas-Alatorre, Mater Lett., 2007, 61, 4447.

9 S. L. R. Barker, D. Ross, M. J. Tarlov, M. Gaitan and L. E. Locascio, Anal. Chem., 2000, 72, 5925.

10 A. Kikuchi and T. Okano, Adv. Drug Delivery Rev., 2002, 54, 53.

11 S. K. Li and A. D'Emanuele, J. Controlled Release., 2001, 75, 55.

12 J. Kost and R. Langer, Adv. Drug Delivery Rev., 2001, 46, 125.

13 N. Peppas, Curr. Opin. Colloid Interface Sci., 1997, 2, 531.

14 L. K. Ista and G. P. Lopez, J. Ind. Microbiol. Biotechnol., 1998, 20, 121.

15 M. Yamato, C. Konno, M. Utsumi, A. Kikuchi and T. Okano, Biomaterials., 2002, 23, 561.

16 J. Hoffmann, M. Plotner, D. Kuckling and W. J. Fischer, Sens. Actuators, A., 1999, 77, 139.

17 D. W. Urry, Biopolymers., 1998, 47, 167.

18 D. E. Owens III, Y. Jian, J. E. Fang, B. V. Slaughter, Y. H. Chen and N. A. Peppas, Macromolecules., 200 7, 40, 7306.

19 T. Sun, G. Wang, L. Feng, B. Liu, Y. Ma, L. Jiang and D. Zhu, Angew. Chem. Int. Ed., 2004, 43, 357.

20 Pankhurst, Q. A. Connolly, J. Jones, S. K. Dobson, J. J. Phys. D: Appl. Phys., 36(2003) R167–R181.

21 Qin, J. Laurent, S. Jo,Y. S.;Roch,A. Mikhaylova,M. Bhujwalla, Z. M. Muller, R. N. Muhammed, M. Adv. Mater., 19 (2007) 1874–1878.

22 Qin, J. Asempah, I. Laurent, S. Fornara, A. Muller, R. N. Muhammed, M. Adv. Mater., 21 (2009) 1354–1357.

23 Ikkai F (2004). L'Oreal, Japan Patent Disclos; 2004–099789.

24 Ikkai F, Adachi E. Macromol Rapid Commun., 2004, 25, 1514.

25 Fumiyoshi Ikkai, Satoshi Iwamoto, Eiki Adachi, Mitsutoshi Nakajima, Colloid Polym Sci., 2005, 283, 1149–1153

26 Patrick Schexnailder and Gudrun Schmidt, Colloid Polym Sci. 2009, 287, 1–11.

27 Wang C, Flynn NT, Langer R. Adv Mater., 2004, 16, 1074–1079.

28 Sahiner N, Colloid Polym Sci., 2006, 285, 283–292.

29 Cohen Stuart MA, Colloid Polym Sci., 2008, 286, 855–864.

30 Satarkar NS, Hilt ZJ, Acta Biomaterialia., 2008, 4, 11–16.

31 Liu T-Y, Hu S-H, Liu K-H, Liu D-M, Chen S-Y, J Control Release., 2008, 126, 228–236.

32 Sunderland CJ, Steiert M, Talmadge J E, Derfus AM, Barry S E, Drug Dev Res., 2006, 67, 70–93.

33 Y. Y. Liu and X.D. Fan, Polymer., 2002, 43, 4997.

34 Y. Wang, J. F. Wong, X. Z. Lin and H. Yang, Nano Lett., 2003, 3, 1555.

35 Y. Deng, W. Yang, C. Wang and S. Fu, Adv. Mater., 2003, 15, 1729.

36 X. Liu, M. D. Kaminski, Y. Guan, H. Chen, H. Liu and A. J. Rosengart, J. Magn. Magn. Mater., 2006, 306, 248.

37 L. Han, S. Li, Y. Yang, F. Zhao, J. Huang and J. Chang, J. Magn. Magn. Mater., 2007, 313, 236.

38 N. Wu, L. Fu, M. Su, M. Aslam, K. C. Wong and V. P. Dravid, Nano Lett., 2004, 4, 383.

39 X. Liu, M. D. Kaminski, Y. Guan, H. Chen, H. Liu and A J. Rosengart, J. Magn. Magn. Mater., 2006, 306, 248.

40 Y. Wang, B. Li. Y. Zhou and D. Jia, Nanoscale Res. Lett., 2009, 4, 1041.

41 L. X. Song, C. F. Teng, P. Xu, H. M. Wang, Z. Q. Zhang and Q. Liu, J. Incl. Phenom. Macrocycl. Chem., 2 008, 60, 223.

42 H. G. Schild, J. Polym. Sci. Part A: Polym. Chem., 1996, 34, 2259.

43 E. Kneller, Theory of the magnetization curve of small crystals, in: H.P.J. Wijn (Ed.), Encyclopedia of Phy sics, Ferromagnetism, Springer, New York, 1966, vol. XVIII/2, p 438–544.

44 R. Hergt, W. Andr, C. G. d'Ambly, I. Hilger, W. A. Kaiser, U. Richter and H. G. Schmidt., IEEE Trans. M agn., 1998, 34, 3745.

45 M. Mary, in scientific and clinical applications of magnetic carriers, ed. U. Hafeli, W. Schutt, and M. Zboro wski). Plenum press, New York, 1997, pp. 303.

46 J. X. Jie, L. Liu, R. Xie, N. Hui and C. L. Yin, Polymer., 2009, 50, 922.

47 Dipti Singh, Dirk Kuckling, Poly.Adv. Technol., 17 (2006) 186-192)4] Y. Wang, J. F. Wong, X. Z. Lin and H. Yang, Nano Lett., 2003, 3, 1555-1559.